

- (2) Iannelli, P.; Immirzi, A. *Macromolecules* 1989, 22, 200.
- (3) Makowski, L. *Fiber Diffraction Methods*; French & Gardner, Ed.; ACS Symposium Series 141; American Chemical Society: Washington, DC, 1980; Chapter 8, p 139.
- (4) Fraser, R. D. B.; MacRae, T. P.; Miller, A.; Rowlands, R. J. *J. Appl. Cryst.* 1976, 9, 81.
- (5) Millane, R.; Arnott, S. *J. Macromol. Sci., Phys.* 1985-1986, B24 (1-4), 193.
- (6) Iannelli, P.; Immirzi, A. *Macromolecules* 1989, 22, 196.
- (7) Immirzi, A.; Iannelli, P. *Gazz. Chim. Ital.* 1987, 117, 201.
- (8) Vainshtein, *Diffraction of X-ray by Chain Molecules*; Elsevier Publishing Company: Amsterdam, The Netherlands, 1966; p 344.
- (9) Holmes, K. C.; Barrington Leigh, J. *Acta Crystallogr.* 1974, A30, 635.
- (10) Fraser, R. D. B.; Suzuki, E.; MacRae, T. P. *Structure of Crystalline Polymers*; Elsevier Applied Science Publishers: Hall, I., Ed.; Chapter 1, p 1.
- (11) Abramowitz, Stegun, *Handbook of Mathematical Functions*, Dover Publications, Inc.: New York, 1970; p 303.
- (12) Morosoff, N.; Sakaoku, K.; Peterlin, K. *J. Polym. Sci., Part A-2* 1972, 10, 1221.

Time-Resolved Small-Angle X-ray Scattering of a High Density Polyethylene/Low Density Polyethylene Blend

H. H. Song,[†] D. Q. Wu,[†] B. Chu,^{*†} M. Satkowski,[‡] M. Ree,[‡] R. S. Stein,[‡] and J. C. Phillips[§]

Department of Chemistry, State University of New York at Stony Brook, Long Island, New York 11794-3400, Polymer Research Institute, University of Massachusetts, Amherst, Massachusetts 01003, and SUNY Beamline X3, NSLS, Brookhaven National Laboratories, Upton, New York 11970. Received May 11, 1989;
Revised Manuscript Received August 1, 1989

ABSTRACT: The semicrystalline morphology of a 50/50 blend of high density polyethylene/low density polyethylene (HDPE/LDPE) was studied by time-resolved small-angle X-ray scattering (SAXS) using the State University of New York (SUNY) Beamline at the National Synchrotron Light Source (NSLS). The HDPE/LDPE blend, which was cooled slowly at a cooling rate of 0.3 °C/min, showed an interfibrillar scale separation within the spherulites that contained both the HDPE and the LDPE component. On the other hand, the same polymer blend, which was cooled rapidly at a cooling rate of 110 °C/min, appeared to show separation of HDPE and LDPE on an interlamellar scale. When the blend was quickly cooled to two successive temperatures, the scattering profiles were similar in nature to those obtained from the same sample that was directly quenched. The two-step rapid cooling represented quenching (1) from ~125 °C, which was above the HDPE crystallization temperature, to 110 °C, which was lower than the HDPE crystallization temperature but higher than the LDPE crystallization temperature, and (2) from 110 to 100 °C, which was below the LDPE crystallization temperature, while the direct rapid cooling was from 135 to 65 °C.

Introduction

Fractionation is known to occur when a polydisperse polymer undergoes crystallization.¹⁻⁴ Such a phenomenon is also seen in quasi-binary polymer pairs.⁵⁻⁹ Of particular interest is the structural arrangement of the two components in a binary blend. Small-angle X-ray scattering (SAXS) can be used to measure the lamellar structure in crystalline polymers. The advent of a higher intensity synchrotron X-ray source⁹⁻¹¹ has made the SAXS technique even more powerful since the crystallization behavior can be studied in the time-resolved mode.

Shultz¹² studied the crystallization of linear polyethylene (LPE) by SAXS. At low crystallization temperatures, the long periods formed by LPE were independent of time. At higher crystallization temperatures, the long periods decreased with time, indicating the formation of new crystallites between the earlier formed lamellae. Rault¹³ et al. studied a 50/50 blend of high density

polyethylene (HDPE) and low density polyethylene (LDPE) by static SAXS. They described the scattering in terms of a paracrystalline model having a bimodal distribution of crystalline widths.

In our previous study⁹ with synchrotron radiation, the lamellar structure of a 50/50 blend of HDPE and LDPE was observed during crystallization under fast cooling (110 °C/min). The results showed that for all three samples (HDPE, LDPE, and 50/50 blend) the lamellar spacing decreased during crystallization and was accompanied by the appearance of a marked hump in the SAXS patterns. The results were interpreted in terms of the ordering of the lamellar structure and the growth of new crystallites in the amorphous zones between the lamellae. In the 50/50 blend, the SAXS results suggested that HDPE and LDPE crystallized separately on an interlamellar scale. In this study we extend our previous SAXS work to two different crystallization conditions. In the first case, the blend was crystallized at a slow cooling rate (0.3 °C/min). Under the second condition, the blend was isothermally crystallized at two different temperatures, T_H and T_L in succession (110 °C/min) where T_H denotes a temperature lower than the crystallization temperature of HDPE but still high enough to keep LDPE in the melt

* Author to whom all correspondence should be addressed.

[†] State University of New York at Stony Brook.

[‡] University of Massachusetts.

[§] Brookhaven National Laboratories.

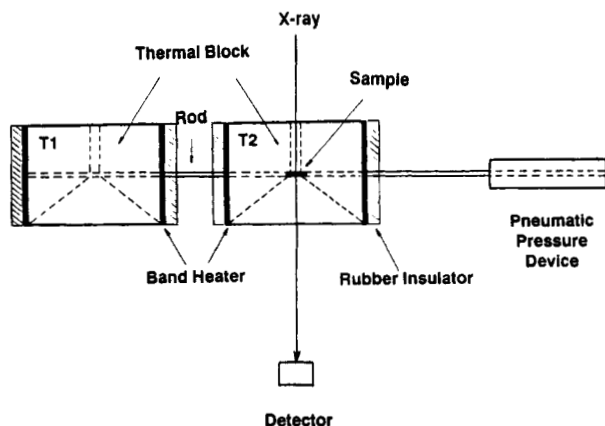


Figure 1. Schematic diagram of thermal blocks for temperature-jump measurements.

state and T_L is low enough to initiate the crystallization of LDPE.

Experimental Section

Materials. The polymers used in this work are the same HDPE, LDPE, and 50/50 HDPE/LDPE blend (by weight percentage) as reported previously.⁹ The HDPE has $M_w = 1.6 \times 10^5$ g/mol and $M_w/M_n \approx 7.1$ with 1 short chain branch per 1000 carbons and a density of 0.957 g/cm³. The LDPE has $M_w = 2.86 \times 10^5$ g/mol and $M_w/M_n \approx 16$ with 26 short chain branches per 1000 carbons and a density of 0.920 g/cm³.

The blend was prepared by dissolving equal weights of HDPE and LDPE in *p*-xylene. The concentration of the solution was 2 g/100 mL. In order to inhibit oxidation, a small amount of 2,6-di-*tert*-butyl-4-methylphenol (1 wt % of PE) was added. The solution was stirred for 1 h at 130 °C. The polymer was precipitated in cold methanol and allowed to dry for 2 days in a vacuum oven at 50 °C. The samples were annealed at 150 °C for ~20 min before SAXS measurements, making sure that no bubbles were present.

SAXS Measurements. SAXS experiments were conducted at the SUNY X21A (or X3A at present) Beamline, NSLS, Brookhaven National Laboratories (BNL) using a modified Kratky block collimation system.¹⁴ We used an X-ray wavelength of 0.154 nm and a beam cross-section at the sample of $\sim 1.5 \times 0.5$ mm². The scattered intensity was collected by a linear position sensitive photodiode array detector (EG&G, Princeton Applied Research, Model 1453) coupled to an optical multichannel analyzer system (EG&G, PAR, Model 1461). The scattering profiles were corrected for detector nonuniformity, sample absorption, background, and incident X-ray intensity fluctuations.

A specially designed thermal sample holder was used to achieve a rapid temperature jump. As shown in Figure 1, the device consisted of two large thermal chambers kept at the desired temperatures T_1 and T_2 . The copper sample cell could be transferred rapidly from one chamber (T_1) to the other (T_2) by means of a metal rod connected to a pneumatic pressure device. Each polymer sample was 6.4 mm in diameter and 2.6 mm thick. The sample was filled into the copper sample cell and contained between two 25- μ m-thick Kapton films. The temperature changes in the quenching experiments were calibrated separately by inserting a thermistor directly into the copper sample cell in the presence of polyethylene polymers. After the sample reached the temperature T_2 , the X-ray measurement was started. The time for the sample to reach an equilibrium temperature at T_2 was thus dependent on the magnitude of the temperature difference ($\Delta T = |T_2 - T_1|$). For example, with $\Delta T = 25$ °C, the sample could reach T_2 in ~20 s.

Results and Discussion

1. Slow Cooling. In the first series of experiments, HDPE, LDPE, and the blend were cooled at a constant

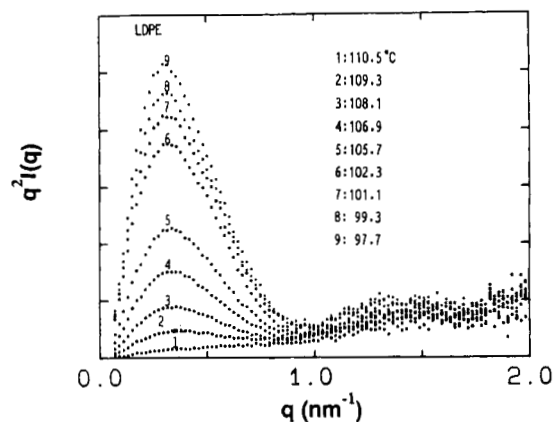


Figure 2. Lorentz-corrected SAXS intensities of LDPE during slow cooling (0.3 °C/min). Each intensity curve has been collected for a period of 10 s.

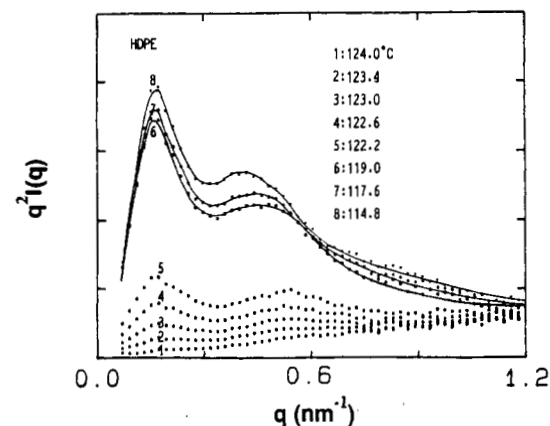


Figure 3. Lorentz-corrected SAXS intensities of HDPE during slow cooling (0.3 °C/min). Each intensity curve has been collected for a period of 10 s.

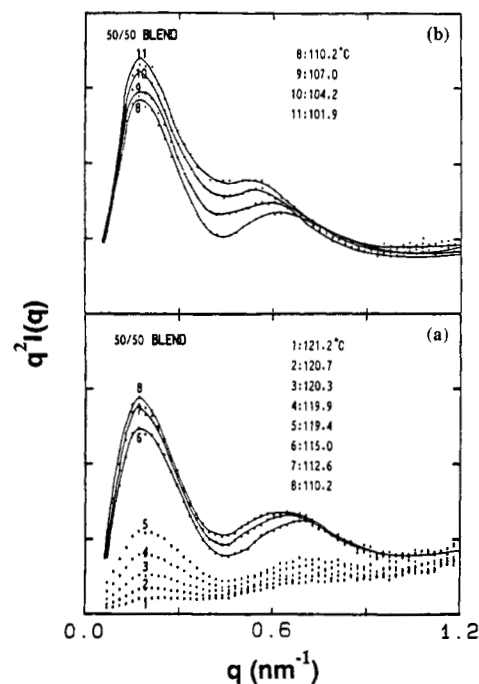


Figure 4. Lorentz-corrected SAXS intensities of the 50/50 HDPE/LDPE blend during slow cooling (0.3 °C/min). Each curve has been collected for a period of 10 s. The curves are partitioned into two groups (a) and (b) for clarity.

rate (0.3 °C/min). Figures 2–4a,b show some of the Lorentz-corrected scattering patterns. Each scattering curve was accumulated for a 10-s period. It is interest-

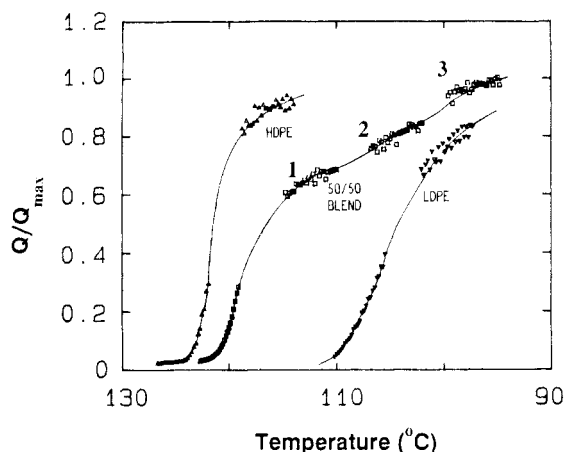


Figure 5. Plot of normalized integrated SAXS intensity, Q/Q_{\max} , vs temperature.

ing to note that both the HDPE and the 50/50 blend show two distinct maxima even early in the crystallization process. The second-order SAXS peak in crystalline polymers, as shown in Figures 3 and 4 over $0.3 \lesssim q \lesssim 0.6 \text{ nm}^{-1}$, is generally seen in systems with a narrow distribution of crystalline and amorphous widths and in systems with a high degree of crystallinity.^{15,16}

From Figures 2–4, the integrated SAXS intensities, Q , normalized by Q_{\max} , are plotted as a function of temperature, as shown in Figure 5. For a two-phase system with sharp phase boundaries Q is given by¹⁷

$$Q = 4\pi \int_0^\infty I(q)q^2 dq = 8\pi^3(\rho_c - \rho_a)^2\phi_c(1 - \phi_c) \quad (1)$$

where ρ_c and ρ_a are the densities of the crystalline and amorphous phases, ϕ_c denotes the degree of crystallinity, and $q = 4\pi \sin \theta / \lambda$, with 2θ being the scattering angle, and λ , the X-ray wavelength. Q_{\max} denotes the maximum value of Q for each set of experiment. In Figure 5, both homopolymers exhibit S-shaped curves. However, for the blend, the normalized integrated SAXS intensity (Q/Q_{\max}) shows a two-step increase. The behavior is due to the separate crystallization of HDPE and LDPE. The 50/50 blend curve can be separated into three regimes. (1) From 120 to 110 °C, Q/Q_{\max} rises rapidly to a plateau at ~ 116 °C and HDPE is being crystallized. (2) From 110 to 100 °C, HDPE continues and LDPE starts to crystallize. (3) From 100 to 90 °C, LDPE dominates the crystallization process.

The stepwise behavior of Q/Q_{\max} for the blend suggested that no cocrystallization occurred between HDPE and LDPE when the polymer blend was being cooled slowly, i.e., at a cooling rate of 0.3 °C/min. With the HDPE and the LDPE forming different crystallites, three basic types of morphologies are then conceivable. (1) Each component crystallizes into separate spherulites of pure HDPE or LDPE. (2) The HDPE and the LDPE form in separate lamellae within the same spherulite. The segregation scale is interlamellar, and the lamellae of HDPE and LDPE are mixed together. (3) The HDPE and the LDPE form separate lamellae within the same spherulite, but in this case the lamellae form stacks or bundles of primarily HDPE or LDPE.

On the basis of the recent study of HDPE/LDPE blends by Ree and Stein,⁸ the first type can be rejected. Differential scanning calorimetry and small-angle light scattering showed that, in slowly cooled (2 °C/min) blends, the entire sample volume was first filled with open spherulites of HDPE and then LDPE crystallized within the previously formed spherulites. We need to turn our atten-

tion to differentiating between cases 2 and 3, i.e., whether the lamellae of HDPE and LDPE are intermixed or segregated into stacks of primarily HDPE or LDPE.

The SAXS scattering profiles from the above two cases are expected to be quite different. If the lamellae are in bundles of a single component (case 3) and these bundles are relatively large in spatial extent, there should be little interference in SAXS region between the large stacks. Then the patterns should be a superposition of scattering from HDPE and LDPE homopolymers. The interfibrillar segregation should also contribute to the forward scattering, depending on the size scale of the segregation. If the size of the interfibrillar regions is comparable to lamellar spacings, the small-angle X-ray scattering could appear in the same q regime due to lamellar scattering.

For the second case, a number of different profiles could result depending on the exact type of separation of HDPE and LDPE. If the HDPE and the LDPE lamellae are intermixed and alternating, the scattering observed would arise from an average of the lamellar widths of HDPE and LDPE. This type of scattering can be modeled using the paracrystalline statistics of Rault et al.¹³ However, the LDPE might still crystallize between the HDPE lamellae but not in lamellar form because of the spatial constraints between the previously formed HDPE lamellae. Then, the small LDPE crystallites might act to raise the electron density in the area between the HDPE lamellae. This effect could manifest itself in changes in Q/Q_{\max} .

When the SAXS intensities of the blend (Figure 4a,b) are compared with those of LDPE (Figure 2) and HDPE (Figure 3), the blend scattering at first seems to resemble that of an intermixed lamellae morphology. The broad first maximum (large peak) and the position of both maxima appear to be from some sort of average of lamellar spacings. However, on closer examination, the scattering profiles show a segregation of bundles of lamellae, which are primarily HDPE or LDPE. This conclusion is suggested by a number of observations. By examining the position of the first maximum, one notes that it is nearly constant from 123 to 101 °C. When we recall that from Figure 5 the crystallization of the blend is a two-step process, the pattern down to 110 °C is primarily HDPE crystallization. If at lower temperatures the LDPE were to crystallize into lamellae between the already formed HDPE lamellae, the more closely spaced LDPE lamellae would result in a marked decrease in the overall long period exhibited in the first maximum; i.e., the scattering peak position would shift to large scattering angles. No such shift was seen in Figure 4. Another observation that could point to segregation of the HDPE and the LDPE lamellae into separate bundles is the presence of a second scattering maximum. According to Hoseman's theory of paracrystallinity,¹⁵ the magnitude of the second-order peak depends on the degree of crystallinity and the breadth of the distribution of lamellar spacing widths. If the LDPE were crystallizing between the HDPE lamellae, the distribution of the overall lamellar spacing widths would broaden severely. The LDPE characteristically shows no second-order peak. Then, one might expect the second-order peak of the cooling blend to decrease when the LDPE was brought to crystallize. This was not observed as the scattering patterns showed a prominent second maximum down to 104 °C. Note that, in the first phase of cooling (125–110 °C) of the blend, where the HDPE crystallization occurred, the heights of the two maxima grew monotonically. In the next stage of cool-

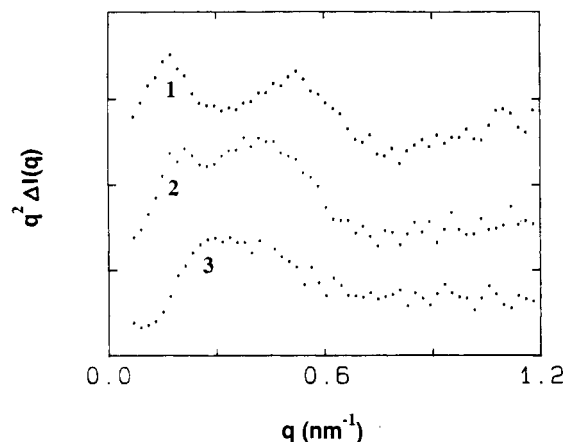


Figure 6. Net SAXS intensity change ($\Delta I(q) \times q^2$) of the 50/50 blend of HDPE/LDPE (Figure 4) during a temperature decrease of $\sim 5^\circ\text{C}$ at the regions 1-3 in Figure 5. Curve 1 denotes the amount of intensity change from 115.0 to 110.2 $^\circ\text{C}$; curve 2 denotes that from 107.0 to 101.9 $^\circ\text{C}$; curve 3 denotes that from 99.8 to 95.0 $^\circ\text{C}$. Each curve is shifted arbitrarily for clarity.

ing when the LDPE crystallization process occurred, the intensity at angles between the two maxima seemed to increase. In order to study this increase further, the net intensity changes at different temperature regions were calculated and plotted in Figure 6. The three temperature regions were chosen as shown in Figure 5: (1) $110^\circ\text{C} < T < 125^\circ\text{C}$, where HDPE crystallized, (2) $100^\circ\text{C} < T < 110^\circ\text{C}$, where LDPE and HDPE crystallized, and (3) $T < 100^\circ\text{C}$, where mostly LDPE crystallized. Each curve in Figure 6 represents the amount of intensity change between two scattering curves at temperatures 5°C apart. Curves 1 and 3 in Figure 6 resemble the SAXS patterns of the HDPE and the LDPE homopolymer, respectively. Curve 2 shows a mixed pattern of each homopolymer. Such a decomposition of SAXS intensities of the blend into the profiles of two homopolymers strongly suggests that the 50/50 HDPE/LDPE polymer blend crystallized to form mostly bundles of HDPE lamellae and LDPE lamellae.

2. Isothermal Crystallization at Two Successive Temperatures. In a previous set of experiments,⁹ the crystallization of the 50/50 HDPE/LDPE blend was studied under rapid cooling ($110^\circ\text{C}/\text{min}$). The results suggested that the lamellae of different PE were not separated into bundles of HDPE lamellae and LDPE lamellae but were mixed together. To further study the behavior of the blend under fast cooling, the same blend was subjected to two rapid decrease in temperature. The blend, initially kept at 150°C in order to remove thermal history, was brought down to $\sim 125^\circ\text{C}$ and then quickly cooled to 110°C . At 110°C , only the HDPE component of the blend was expected to crystallize. The sample was then cooled to 100°C at which temperature the LDPE would crystallize. By means of this two-step cooling process, contributions to the scattering by HDPE and LDPE can be separated.

Figure 7a shows selected Lorentz-corrected SAXS intensities measured during the first step of the crystallization at 110°C . The curves show only a single peak, which grows in the usual manner. After the temperature was lowered to 100°C , the LDPE began to crystallize. The resulting scattering profiles are shown typically in Figure 7b. The shift in peak position from small to larger scattering angles suggests that LDPE is being crystallized between the previously formed HDPE lamellae. A similar shift was observed for the same sample that was rapidly cooled from ~ 135 to 65°C .⁹ Thus, the same

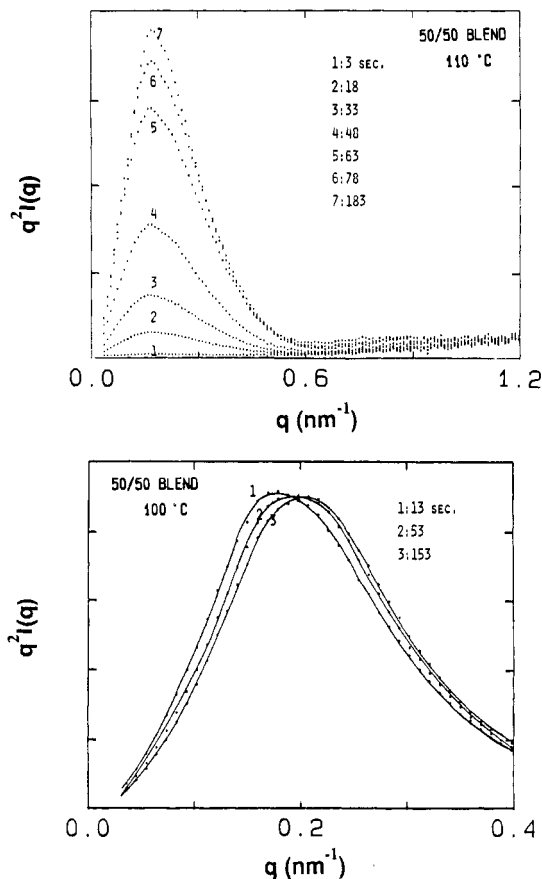


Figure 7. (a) Lorentz-corrected intensity of the 50/50 HDPE/LDPE blend measured during the isothermal crystallization at 110°C . Each SAXS curve represents a 5-s collection time. (b) Lorentz-corrected intensity of 50/50 HDPE/LDPE blend measured during the isothermal crystallization at 100°C , after the blend has been crystallized at 110°C for 45 min. Each SAXS curve represents a 5-s collection time.

conclusion can be drawn for a rapid two-step crystallization as for the rapid one-step crystallization; i.e., during rapid quenching lamellae of HDPE and of LDPE are mixed together, while there is evidence for the formation of bundles of HDPE lamellae and LDPE lamellae in the slow cooling process ($0.3^\circ\text{C}/\text{min}$).

Conclusion

Upon slow cooling ($0.3^\circ\text{C}/\text{min}$), small-angle X-ray scattering intensity profiles observed during the crystallization of a 50/50 HDPE/LDPE blend suggested the formation of separate bundles of HDPE lamellae and LDPE lamellae. Patterns taken at 120 – 110°C resembled the HDPE homopolymer scattering, while those taken at 100 – 90°C resembled the LDPE homopolymer scattering. Between 110 and 100°C , the scattering pattern appeared to be a superposition of those from both HDPE and LDPE. Such a decomposition of the SAXS intensities into SAXS patterns of HDPE and LDPE homopolymers would be typical of segregation of bundles of lamellae on an inter-fibrillar scale.

Isothermal crystallization of the blend at two successive temperatures (110 and 100°C) produced a morphology where the lamellae of HDPE and of LDPE might be mixed together, similar to the interlamellar separation of HDPE and LDPE components in a rapidly cooled ($110^\circ\text{C}/\text{min}$) blend.

Further work on this system will include SAXS studies of the composition dependence of the lamellar structure.

Acknowledgment. B.C. gratefully acknowledges the support of this research by the U.S. Department of Energy (DEFG0286-ER45237A003). The authors from the University of Massachusetts appreciate the support of the Division of Materials Research of the National Science Foundation and of the Materials Research Laboratory of the University of Massachusetts. The assistance of Exxon Chemical Co. in providing samples is gratefully appreciated as are discussions with Dr. Ferd Stehling of Exxon and Prof. Leo Mandelkern of Florida State University. The work was carried out at the SUNY Beamline supported by the U.S. Department of Energy (DEFG0286-ER45231A003) at the National Synchrotron Light Source, Brookhaven National Laboratories, which is sponsored by the U.S. Department of Energy under Contract DE-AC02-76CH00016.

References and Notes

- (1) Bunn, C. W.; Cobbold, A. J.; Palmer, R. P. *J. Polym. Sci.* **1958**, *28*, 365.
- (2) Keith, H. D.; Padden, F. J. *J. Appl. Phys.* **1964**, *35*, 1270 and 1286.
- (3) Geil, P. H.; Anderson, F. R.; Wunderlich, B.; Arakawa, T. *J. Polym. Sci.* **1964**, *2*, 3707.
- (4) Metha, A.; Manley, R. *Colloid Polym. Sci.* **1975**, *253*, 193.
- (5) Smith, P.; Manley, R. *Macromolecules* **1979**, *12*, 483.
- (6) Shu, P. H. C.; Burchell, D. J.; Hsu, S. L. *J. Polym. Sci.* **1980**, *18*, 1421.
- (7) Hu, S. R.; Kyu, T.; Stein, R. S. *J. Polym. Sci.* **1987**, *25*, 71.
- (8) Ree, M.; Stein, R. S., to be published.
- (9) Song, H. H.; Stein, R. S.; Wu, D. Q.; Ree, M.; Phillips, J. C.; LeGrand, A.; Chu, B. *Macromolecules* **1988**, *21*, 1180.
- (10) Russell, T. P.; Koberstein, J. T. *J. Polym. Sci.* **1985**, *23*, 1109.
- (11) Ungar, G.; Keller, A. *Polymer* **1986**, *27*, 1835.
- (12) Shultz, J. M. *J. Polym. Sci.* **1976**, *14*, 2291.
- (13) Reckinger, C.; Larbi, F. C.; Rault, J. *J. Macromol. Sci.* **1985**, *B23*, 511.
- (14) Chu, B.; Wu, D. Q.; Wu, C. *Rev. Sci. Instrum.* **1987**, *58* (7), 1158.
- (15) Hoseman, B.; Bagchi, S. N. *Direct Analysis of Diffraction by Matter*; Interscience Publishers: New York, 1962.
- (16) Vonk, C. In *Small Angle Scattering*; Brumberger, H., Ed.; John Wiley: New York, 1977.
- (17) Guinier, A.; Fournet, G. *Small Angle Scattering of X-rays*; John Wiley: New York, 1955.

Registry No. PE, 9002-88-4.

Equilibrium Polarization of Polar Polymers in a Matrix of Arbitrary Compliance

S. Havriliak, Jr.

Rohm and Haas Research Laboratories, P.O. Box 219, Bristol, Pennsylvania 19007.
Received November 3, 1988; Revised Manuscript Received October 25, 1989

ABSTRACT: The assumptions underlying the computer-simulated motions by Mansfield and those by Perchak et al. are extended to the Onsager-Kirkwood theory of polar liquids to develop a model for polar polymers in a rigid environment. This extension is made by expanding the perturbed Hamiltonian of the system upon application of the electric field to include a strain energy term. The strain energy term arises because any finite orientation of polar groups in an electric field must also distort the system. The resulting distortion will cause the strain energy term to be finite because the equilibrium tensile compliance is not, in general, infinite for polymers as it is for polar liquids. Two cases are considered: The first one converges to the Onsager-Kirkwood results as the tensile compliance approaches infinity (i.e., strain energy is zero) and their reaction field is an adequate representation for long-range interactions. The second case assumes the tensile compliance to be finite, the point dipole to be located on a nonspherical molecular segment, and the reaction field not to be an adequate representation of long-range interactions. Under these assumptions, a Debye-like expression is obtained. However, unlike Debye's expression, a Curie point is not observed because the orientation process is inhibited by means of the finite strain energy.

Introduction

Mansfield¹ proposed a spring and dash pot model to represent intramolecular and intermolecular interactions in polymers and then calculated the loci of the dielectric relaxation process when represented in a complex plane for a range of model parameters. The significance of his calculation is that these complex plane loci are similar to those observed experimentally, a feature not obtained with any other polymer model. Most polymer chain models have molecular weight dependent shapes that are very narrow when compared to those observed experimentally. One interpretation of the dash pot connecting the polymer chain to the environment in Mansfield's model is that it represents the rigidity of the environment inhibiting the orientation process. More recently, Perchak et al.² computer-simulated the ring-flip motions

(β -process) observed in the glass phase of polycarbonate. He found that a rigid lattice prevented the orientation process from taking place while flexible ones permitted them. It is the purpose of this work to generalize these inhibition mechanisms of the environment on the orientation process of polymer chains in the polar liquid theories on Onsager³ and Kirkwood,⁴ hereafter designated as O-K.⁵

O-K assumes polar liquids to be adequately represented by a collection of point dipoles in a microsphere that represents the local structure of a polar liquid. The medium outside this microsphere is considered to be adequately represented by the macroscopic dielectric constant, ϵ_0 . When the electric field is turned on, the energy (Hamiltonian = $H^0(p,q)$) of the system is reduced (perturbation term to the Hamiltonian = $H'(p,q)$) by a reshuffling of the local structures to form a net dipole moment